Open Access Theses   Theses and Dissertations

Fall 2014

Effects of Hip and Ankle Moments on Running Stability: Simulation of a Simplified Model

Rubin C. Cholera
Purdue University

Follow this and additional works at: https://docs.lib.purdue.edu/open_access_theses

Part of the Biomechanics and Biotransport Commons, Mechanical Engineering Commons, and the Robotics Commons

PURDUE UNIVERSITY
GRADUATE SCHOOL
Thesis/Dissertation Acceptance

This is to certify that the thesis/dissertation prepared

By Rubin C Cholera

Entitled
Effects of Hip and Ankle Moments on Running Stability: Simulation of a Simplified Model

For the degree of   Master of Science in Mechanical Engineering

Is approved by the final examining committee:

Dr. Justin E Seipel

Dr. Raymond Cipra

Dr. Xinyan Deng

To the best of my knowledge and as understood by the student in the Thesis/Dissertation Agreement, Publication Delay, and Certification/Disclaimer (Graduate School Form 32), this thesis/dissertation adheres to the provisions of Purdue University's "Policy on Integrity in Research" and the use of copyrighted material.

Dr. Justin E Seipel

Approved by Major Professor(s): _____

Approved by: Dr. Ganesh Subbarayan   12/02/2014

Head of the Department Graduate Program   Date

EFFECTS OF HIP AND ANKLE MOMENTS ON RUNNING STABILITY:

SIMULATION OF A SIMPLIFIED MODEL

A Thesis

Submitted to the Faculty

of

Purdue University

by

Rubin C Cholera

In Partial Fulfillment of the

Requirements for the Degree

of

Master of Science in Mechanical Engineering

December 2014

Purdue University

West Lafayette, Indiana

This is for my parents and my brother who encouraged me to pursue graduate studies

ACKNOWLEDGEMENTS

TABLE OF CONTENTS

LIST OF TABLES

LIST OF FIGURES

ABSTRACT

Cholera, Rubin C. M.S.M.E., Purdue University, December 2014. Effects of Hip and Ankle Moments on Running Stability: Simulation of a Simplified Model. Major Professor: Dr. Justin E Seipel, School of Mechanical Engineering.

In human running, the ankle, knee, and hip moments are known to play different roles to influence the dynamics of locomotion. A recent study of hip moments and several hip-based legged robots have revealed that hip actuation can significantly improve the stability of locomotion, whether controlled or uncontrolled. Ankle moments are expected to also significantly affect running stability, but in a different way than hip moments. Here we seek to advance the current theory of dynamic running and associated legged robots by determining how simple open-loop ankle moments could affect running stability. We simulate a dynamical model, and compare it with a previous study on the role of hip moments. The model is relatively simple with a rigid trunk and a springy leg to represent the effective stiffness of the knee. At the hip we use a previously established proportional and derivative controlled moment with pitching angle as feedback. At the ankle we use the simplest ankle actuation, a constant ankle torque as a rough approximation of the net positive work done by the ankle moment during human locomotion. Even in this simplified model, we find that ankle and hip moments can affect the center of mass (COM) and pitching dynamics in distinct ways. Analysis of the governing equations shows that hip moments can directly influence the upper body

balance, as well as indirectly influence the center of mass translation dynamics. However, ankle moments can only indirectly influence both. Simulation of the governing equations shows that the addition of ankle moment has significant benefits to the quality of locomotion stability, such as a larger basin of attraction. We also find that adding the ankle moments generally expands the range of parameters and velocities for which the model displays stable solutions. Overall, these findings suggest that ankle moments would play a significant role in improving the quality and range of running stability in a system with a rigid trunk and a telescoping leg, which would be a natural extension of current springy leg robots. Further, these results provide insights into the role that ankle moments might play in human locomotion.

1. INTRODUCTION

Bipedal locomotion has been a topic of interest in dynamics, biomechanics, and control as it presents a complicated problem of stabilizing, what is essentially, a multi-segmented inverted pendulum. Understanding bipedal locomotion has potential applications in biomechanics, assistive exoskeletons, prosthetics and robotics. Human motion is affected by joint moment patterns controlled by the central nervous system [1]. These patterns have been analyzed for various movements. The lower extremity of the body is involved in most athletic movements. The major tasks associated with athletic movements have been generalized by Winter and Bishop [2] into four categories:

1. Shock or energy absorption and control of vertical collapse during weight acceptance phase.
2. Balance and posture control of upper body.
3. Energy generation associated with forward and upward propulsion.
4. Control of direction changes of the center of mass of the body.

For level running, when we analyze the motion in the sagittal plane, the first three tasks are considered. Running gait consists of a stance phase and a flight or swing phase. Stance phase begins when the foot comes in contact with the ground and ends when the toe leaves the ground. Stance phase begins with energy absorption and weight acceptance

followed by energy generation to propel the body. Flight or swing phase consists of swinging the leg back into position for the energy absorption phase.

Individual joint moments and powers have been studied to ascertain the roles of each of these moments in carrying out the tasks of running. Hip extensor muscles have been shown to contribute to the dynamic balance of the upper body or head arms and torso (HAT), while also assisting knee extensors in energy absorption and preventing knee collapse [3]. Hip flexor muscles come into play during the end of stance phase to decelerate the hip and prepare for leg swing in flight. Over the entire stride the knee was shown to have five distinct phases of energy absorption and generation, but over the stride the knee muscles absorbed 3.6 times the energy they generated [4]. The role of the knee is primarily energy absorption with a small burst of generation in the end of stance phase. The ankle function during the stance phase is divided into three phases, Controlled Plantarflexion (CP), Controlled Dorsiflexion (CD), and Powered Plantarflexion (PP) [5]. CP is when the heel strikes for touchdown, CD is when the "foot" link is flat on the ground and PP is when the heel lifts off and the toe is touching the ground. Studies have shown that CP is a shock absorption phase, CD is an energy storing phase and PP is the energy generation phase. However the energy generation in PP is much larger than the energy absorbed during CP and CD [4–6]. Over a stride, ankle muscles have been shown to generate 2.9 times the energy absorbed. Also in comparison to the knee, the work done by the ankle plantarflexors averaged three times the work done by knee extensors [4]. Although the ankle muscles are responsible for upper body stability during standing, the task of ankle muscles in gait is some energy absorption with large energy generation towards propulsion.

In another study, the joint moments and powers are compared with respect to speed [7]. Figure 1.1. shows the joint moments and power for different speeds. Ankle power generation was shown to be directly related to speed, also suggesting that the ankle plays the role of propulsion. The knee moment patterns are shown to be similar for running and sprinting speeds, suggesting a more passive role in human running.

Other experimental studies on joint moments in human locomotion [8,9] have also shown that there is a significant ankle actuation for both walking and running gaits. In some studies ankle moment had been approximated by a spring with 'quasi-stiffness' for slow walking speeds. However, the relation between ankle moment and ankle angle became nonlinear with increase in speed [10].

These studies talk about the different roles of joint moments in human locomotion. The conclusions are based on just the joint moment patterns and power calculated from experimental observations like, joint positions, ground reaction forces, and EMG signals. There could be more to the roles of joint moments in legged locomotion that could be found through dynamical modeling and robotics.

In robots, hip moments alone were shown to be sufficient to stabilize both COM translational and pitching dynamics [11,12]. Experiments on controlled below knee ankle-foot prostheses showed better gait and terrain adaptiveness than passive spring-like energy storing prosthesis [13,14]. The study on ankle-foot prostheses suggested that apart from propelling the body in stance, ankle moments also affected COM and pitching stability. The subjects with passive ankle prosthesis also showed a change in hip moment patterns and that changed the gait. This study hinted that energy generating ankle moments had a role in improving stability over passive energy balanced ankle moments.

Currently, there is not a lot of understanding regarding the role of joint moments in dynamic locomotion and most highly dynamic running robots currently in existence have been based on a springy-leg "pogo-stick" theory of locomotion. The state of the art for stable dynamic robots is largely based upon hip-based actuation of otherwise compliant "springy" legs.

The objective of this thesis is to determine the effect of adding an ankle moment to an existing hip-based spring-mass model of running, and in particular determine the following:

1. How hip and ankle moments affect COM and pitching dynamics.

2. How a model with hip and ankle moments react to perturbations in state variables.

3. How hip and ankle moments affect the range of stable parameters of the model.

The eventual goal of this research is to use the knowledge gained from these simulations in the design of better robots. The robots shown in the earlier study [11,12] were hip actuated and had a springy leg. With the results of this study we could design a similar robot with added ankle moments.

Testing the response to perturbations is not something easily done in humans and could also lead to some ethical issues. Quantifying stability effects is very easily done in dynamical simulations and could potentially also be tested in robots.

An approach of dynamical modeling and simulation might give us more specific information on the roles and effects of joint moments in human running. Information that could be hidden in the governing equations or the simulated results. In dynamical modeling we can study the effect of a specific property by isolating it and comparing,

which is not easily done in experiments on humans. For example, we can compare models with and without ankle moments to see the effect of adding ankle moments. We can better quantify the stability in terms of response to perturbations. Mathematical modeling and simulation also allow a better control over the parameter space with applications extending beyond just the human range of parameters

Our modeling approach is to use a simplified dynamical model of human running. We propose a mathematical model with active hip and ankle moments to explore their roles in running stability. We model the knee as a passive damped springy leg for the following reasons:

1. The knee muscles absorbed 3.6 times the energy they generated [4].
2. The knee muscles were shown to contribute three times less work than ankle moments [4].
3. The knee moment patterns were shown to be similar for running and sprinting speeds, suggesting a more passive role in human running [7]
4. Simplicity of model and reducing parameters.

In the next chapter we will detail the approach of using dynamical models to study legged locomotion. In Chapter 3 we present the simplified model along with the governing equations and the analysis methods. In Chapter 4 we present the results, how the results of this model may relate to human running and design of robots. In Chapter 5 we summarize the work and talk about its direct applications in a robot. In the last chapter we make suggestions towards future work.
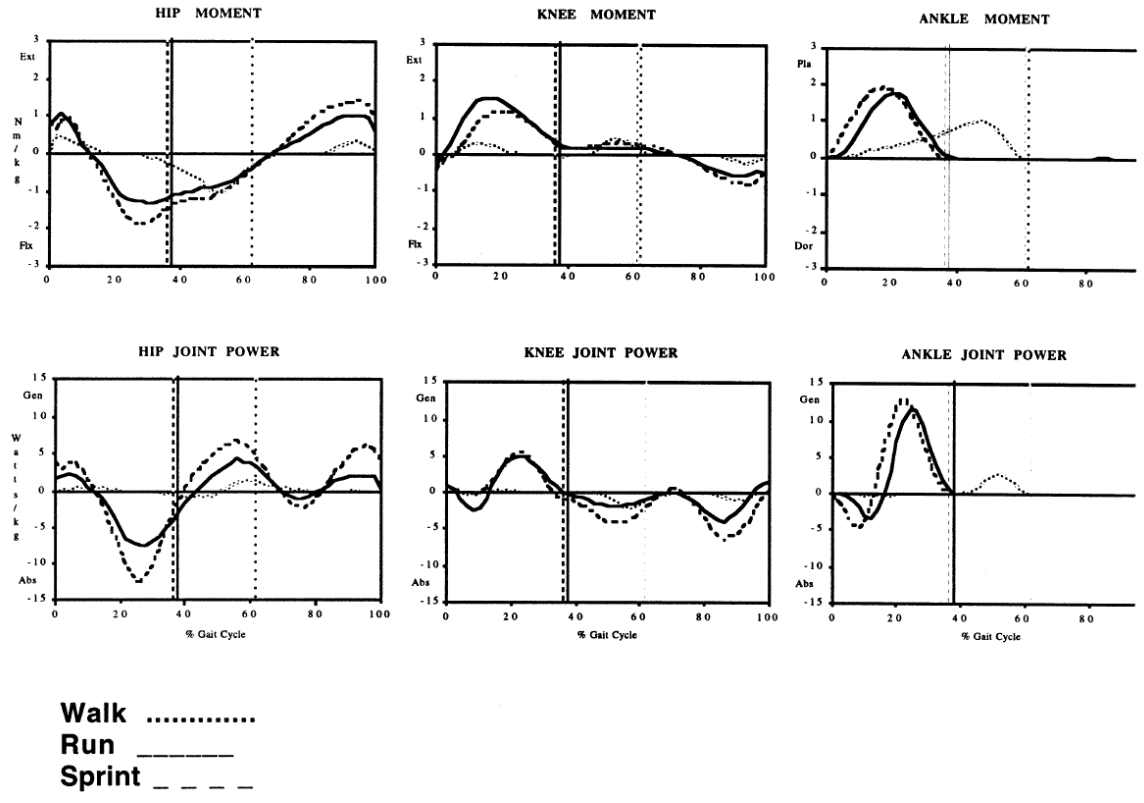
Figure 1.1. Joint moments and power for different speeds based on experimental observations. Image courtesy Tom F. Novacheck [7]

2. APPROACH

Mathematical modeling and simulation has been one of the familiar ways of unraveling the complexity of legged locomotion [15]. The approach taken here to model legged locomotion is based on the concept of templates and anchors [16] which involves using simplified templates which exhibit desired behavior and creating anchors by adding specific aspects of legged locomotion which we wish to study.

2.1   Modeling Background

Simple spring mass systems like the spring loaded inverted pendulum (SLIP) [17,18] have been used reproduce stable center of mass (COM) trajectories displayed by animals. The model consists of a simple point mass joined to a springy leg at the "hip". This was considered a "template" for legged locomotion where the complications like number of legs, symmetry, joints and pitching were reduced to reproduce COM dynamics as seen in animals. Actuation at the hip and damping in the leg was added to the SLIP model to produce robust motion with large perturbation stability [19–21]. A compliant ankle joint when appended to a SLIP model gave rise to asymmetry in landing and take-off about the vertical [22]. The knee joint is commonly approximated by a linear spring due to the nature of the joint moment. A segmented leg SLIP model [23] was shown to have similar stability and COM dynamics as a hip actuated SLIP model. The model replaced the

springy leg by two segments joined by a springy knee. Consistent across all these studies was that there was found some inherent dynamical stability in legged locomotion which helps the system respond to perturbations even when simple feed-forward control approaches were used.

These models simplified the body to a point mass. Humans and human-like robots also have to address trunk pitching stabilization. In humans trunk pitching is known to be stabilized by hip moments. In robots, trunk stabilization is commonly addressed by applying a proportional and derivative (PD) controlled hip moment by measuring its pitching angle with respect to the ground [11,12]. Just a PD controlled torque at the hip was shown to be sufficient to stabilize both COM translational and pitching dynamics. Recently there has been research on SLIP models where the point mass has been replaced by a trunk joined to the leg at the "hip." A modified PD control strategy [24], applied to a simple pitched-actuated SLIP model, based on the angle between the trunk and the leg, was shown to display full asymptotic stability. The control strategy was simple and the only feedback required was the angle between the trunk and leg, which is an internal state variable and easy to implement in robotics. A virtual pivot point (VPP) based scheme [25], applied to a similar trunk pitching based SLIP model with an undamped leg also showed robust stability. Interestingly the hip torque pattern generated by the control scheme was close to the human hip torque in value and shape. However, the control scheme required two feedback variables and is apparently more complex than that typically applied to robotics. These models of locomotion are under-actuated with active actuation only at the "hip" joint and could be used to represent the dynamics of similar robots [11] or special cases of human locomotion like the case of above-knee amputees.

2.2   Modeling and Analysis Approach for This Study

Here, we add an ankle moment to a trunk pitching SLIP model to study the effect of hip and ankle moments on running stability. We propose a model similar to the pitched-actuated SLIP model, with two differences. First, the hip actuation is PD controlled based on the trunk pitching angle with respect to the ground. This is a common trunk balance control strategy used in robotics. Second, we add a moment at the "ankle" joint, where the leg meets the ground.

Due to the nature and role of knee moments detailed in the earlier section we continue to model the knee as a massless springy leg. This approximation has served well as a template for legged locomotion. This allows us to avoid additional parameters like segment lengths and constraints, while allowing us to focus on how hip and ankle actuation work together. We can also make direct comparisons between a previously studied model with just hip moments and the same model with additional ankle moment. Since we do not have a "foot" link in the model, there is no concept of CP, CD and PP. As the energy released by the ankle muscles is much larger than the energy absorbed, we model the net positive work done by the ankle joint as a constant moment at the joint where the springy leg touches the ground. This has the advantage of being a simple feedforward actuation allowing us to isolate the effect of ankle actuation on model dynamics rather than the effect of some feedback control strategy. Also feedforward actuation is easier to apply to robotics.

Later we show how ankle and hip moments affect COM and pitching dynamics in different ways suggesting towards different roles. The model is shown to have full asymptotic stable solutions for human range of parameters in running gait. Addition of

ankle moments significantly improves the qualitative stability of the solution, i.e. response to large perturbations in state variables. It also significantly increases the range of most parameters for which we can find stable solutions, extending beyond the human range making it more suitable for application in robotics. Addition of ankle moments also allowed for solutions with lower running velocities than without ankle moments. We find that the model responds to larger perturbations as we increase the value of ankle moments. We also sample a few more parameters to see if the effects of adding ankle moments repeat. We find that for some parameters the model with ankle moments has a different stable range than with ankle moments, in those cases simply adding ankle moments does not lead to improvement in stability. If those parameters are adjusted to apply to the model with ankle moments we see similar improvement in stability.

3. MODEL

As was briefly introduced in the Approach section, here we will use the hip actuated SLIP model as our template to develop a model that we will use for the rest of this study. To modify the hip actuated SLIP model, we replace the point mass with a rigid trunk that has mass and a rotational moment of inertia, as shown in Figure 3.1.
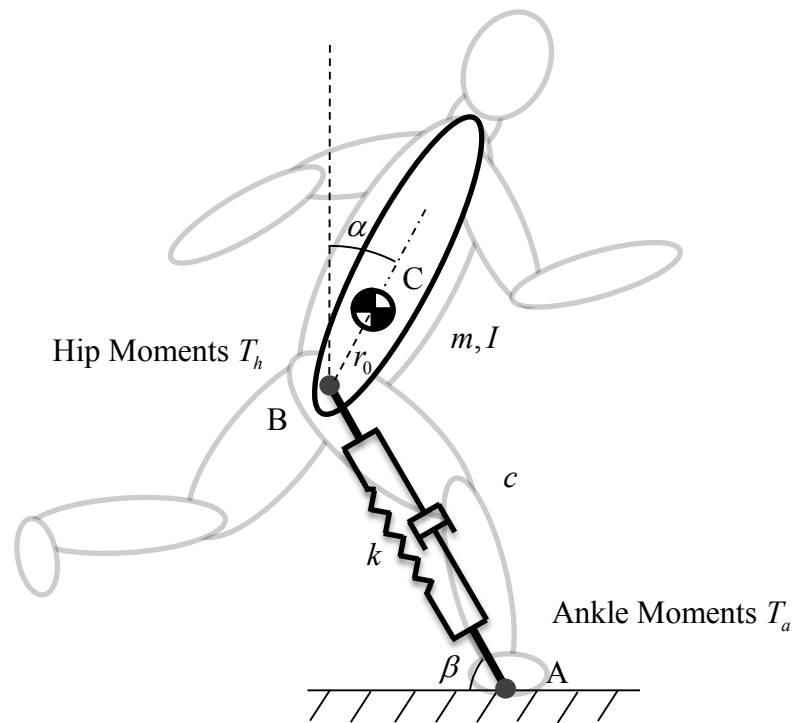
Figure 3.1. SLIP based model of a rigid trunk and a springy leg, powered by hip and ankle moments

The trunk is stabilized by a PD control torque which uses the pitching angle with respect to the ground as feedback. We choose a PD control strategy as it is commonly

used in robotics and it has been shown to stabilize both COM and pitching dynamics. We add another actuation at the joint where the springy leg meets the ground and call it the ankle torque, although that is not truly the ankle joint. The ankle actuation is a constant torque to model the net positive work done by the ankle joint. The model moves in two phases, the stance phase and the flight phase. The stance phase is when the leg is in contact with the ground and the moments do work. When the vertical ground reaction force reaches zero, the model takes off and switches to flight phase where the model is affected only by gravity until the leg touches down again.

3.1 Model Dynamics

The model consists of a massless springy leg AB which has stiffness k, damping c and a rest length of l_0. One end of the leg is pin jointed at the hip to a trunk BC of mass m, moment of inertia about its center of mass of I and the other end is pin jointed to the ground. The center of mass of the trunk is located at a distance of r_0 from the hip joint. There is a constant torque at the ankle T_a and a PD controlled torque at the hip T_h. As the leg is massless, the model has three degrees of freedom defined by the position variables of the center of mass x, y, and α (where positive α is clockwise from the vertical). We define the position of the leg by the coordinates of the ankle $(x_f, 0)$, and angle θ (where positive θ is clockwise from the negative x-axis and x_f is the x-coordinate of the foot).

For the stance phase, the equations of motion will be derived using Newton's laws of motion. The free body diagrams for the model are given below in Figure 3.2.
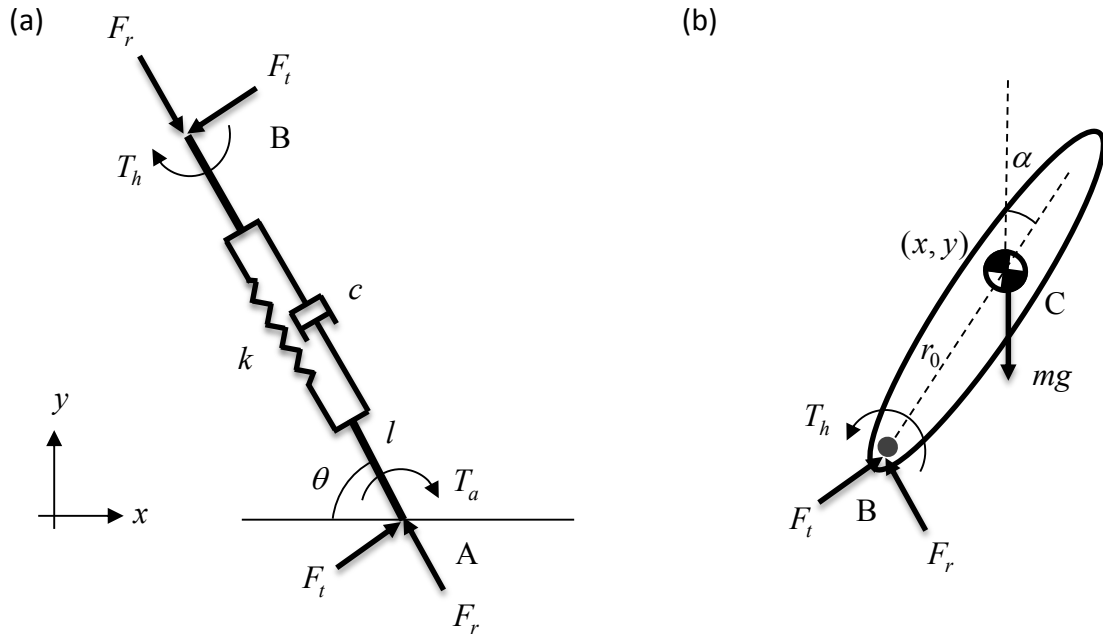
Figure 3.2. (a) Free body diagram of the massless leg. (b) Free body diagram of the trunk.

Balancing the force and torque on the leg gives us

$$F_t = \frac{\left(T_h + T_a\right)}{l} \tag{3.1}$$

$$F_r = k\left(l_0 - l\right) + c\dot{l} \tag{3.2}$$

Where the hip torque is governed by a controller with proportional gain K_p and derivative gain K_d with respect to a reference pitching angle α_r.

$$T_h = K_p\left(\alpha - \alpha_r\right) + K_d\dot{\alpha} \tag{3.3}$$

The leg length and the rate of change of length can be expressed in terms of the coordinates x, y, and α.

$$l = \sqrt{\left(x - r_0 \sin\alpha - x_f\right)^2 + \left(y - r_0 \cos\alpha\right)^2} \tag{3.4}$$

$$l = \frac{\left\{\left(x - r_0 \sin\alpha - x_f\right)\left(\dot{x} - r_0\dot{\alpha}\cos\alpha\right) + \left(y - r_0\cos\alpha\right)\left(\dot{y} + r_0\dot{\alpha}\sin\alpha\right)\right\}}{l} \qquad (3.5)$$

To apply Newton's laws of motion on the trunk, we transform the forces along the leg and perpendicular to the leg, to forces in x and y directions.

$$F_y = F_t \cos\theta + F_r \sin\theta \qquad (3.6)$$

$$F_x = F_t \sin\theta - F_r \cos\theta \qquad (3.7)$$

Where the angle of the leg θ can be expressed in terms of the coordinates x, y, and α.

$$\theta = \cos^{-1}\left(\frac{x_f - x + r_0 \sin\alpha}{l}\right) \qquad (3.8)$$

By Newton's laws of motion, the three equations of motion of the trunk for stance phase are -

$$m\ddot{x} = F_x \qquad (3.9)$$

$$m\ddot{y} = F_y - mg \qquad (3.10)$$

$$I\ddot{\alpha} = F_y r_0 \sin\alpha - F_x r_0 \cos\alpha - T_h \qquad (3.11)$$

During flight phase, the only force on the trunk is gravitational. The center of mass moves in projectile motion and the trunk continues to rotate with the angular velocity at takeoff. In flight we assume that the massless leg returns to its initial angle of β in preparation of the next stance phase. The equation of motion governing the center of mass is –

$$\ddot{y} = -g \qquad (3.12)$$

The condition for switching from stance phase to flight phase, or lift-off (LO), is the vertical ground reaction force becoming zero.

$$LO: F_y = 0 \tag{3.13}$$

The condition for switching from flight phase to stance phase, or touch-down (TD) is when the foot touches down at the fixed landing angle of β.

$$TD: y = r_0 \cos\alpha + l_0 \sin\beta \tag{3.14}$$

After touchdown the new x-coordinate of the foot can be found in terms of the trunk coordinates.

$$x_f = x - r_0 \sin\alpha + l_0 \cos\beta \tag{3.15}$$

3.2 Simulation

The equations of motion are coupled nonlinear differential equations; hence, they cannot be solved exactly. We are looking for stable periodic motion about an unstable equilibrium point (inverted double pendulum) which makes approximate solutions methods like perturbation methods inaccurate. Also there is the added complexity of hybrid dynamics with switching conditions. With these difficulties in mind we use numerical integration to solve these equations as an initial value problem.
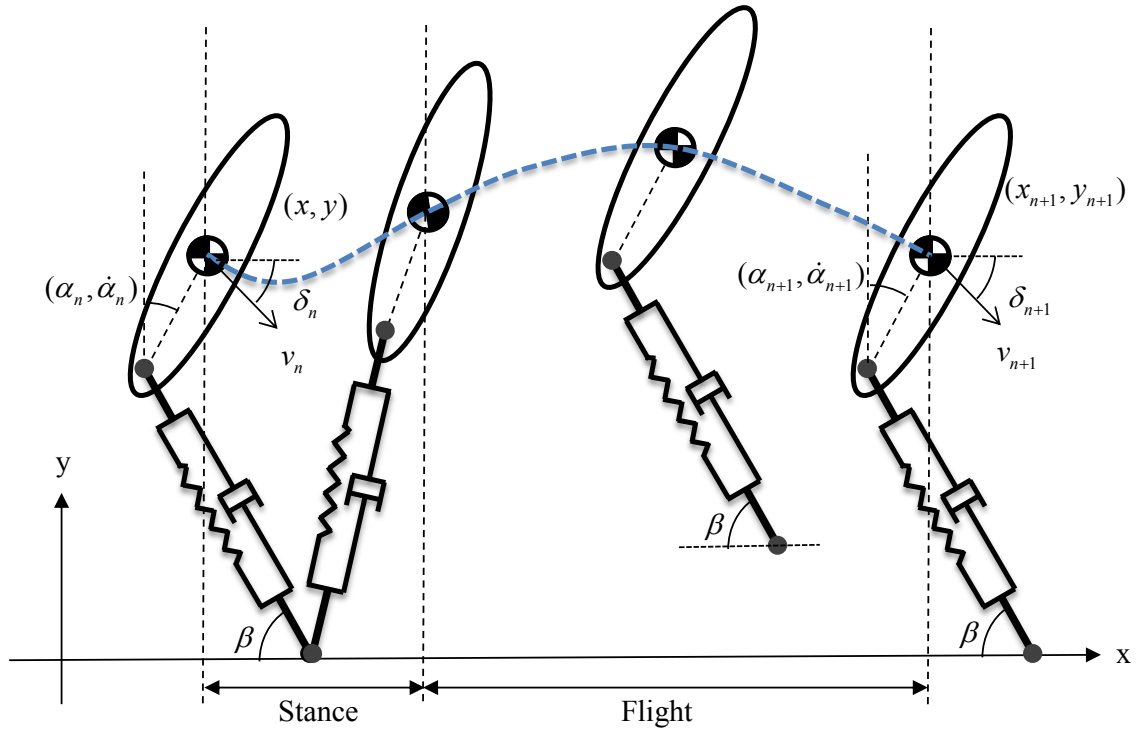
Figure 3.3. Schematic showing one stride of motion.

For the purpose of this paper we shall call those initial conditions which give periodic motion as "fixed points." Not to be confused with the fixed points seen in conventional nonlinear dynamics literature. For this model we say the motion is periodic when the velocity (translational and rotational) and the pitching angle of the $(n+1)^{th}$ touchdown, the nth touchdown, and so on are the same as the initial velocity and pitching angle. Figure 3.3. shows an entire stride from touchdown to touchdown. We define the translational velocity by magnitude v and direction δ (where δ is positive clockwise from the horizontal).

$$v_{n+1} = v_n = v^*, \ \delta_{n+1} = \delta_n = \delta^*, \ \alpha_{n+1} = \alpha_n = \alpha^*, \ \dot{\alpha}_{n+1} = \dot{\alpha}_n = \dot{\alpha}^* \qquad (3.16)$$

We find these fixed points by iteratively solving the equations of motion for a set of parameters while checking for periodicity. Note that the periodicity is dependent on the initial conditions and also all the model parameters. Our goal is to find fixed points for human-like parameters and zero ankle torque. Once we find such a fixed point we add the ankle torque and see how it affects the stability, and the region of stable parameters for the model.

3.3   Qualitative Stability

To compare the quality of stability of fixed points we can plot a basin of attraction by perturbing the state variables and checking if the system returns to the original periodic solution. The four state variables are v, δ, α, $\dot{\alpha}$ and for the purpose of plotting we will split it into a return map of the translational variables (v, δ) and the rotational variables $(\alpha, \dot{\alpha})$.

3.4   Quantitative Stability

To quantify the stability of the system we make a Jacobian matrix corresponding to a numerically approximated four dimensional return map of the state variables. We start off with a fixed point $(v^{*}, \delta^{*}, \alpha^{*}, \dot{\alpha}^{*})$ and perturb one variable by a small amount, say Δv and the values of all the state variables are recorded at the next touchdown $(v_{\Delta v}, \delta_{\Delta v}, \alpha_{\Delta v}, \dot{\alpha}_{\Delta v})$. Similarly we perturb the other variables one by one and get the values of the variables at the next touchdown. Using these values we generate the Jacobian of the return map given by –

$$
J = \begin{bmatrix}
\left(v_{\Delta v} - v^*\right)\big/\Delta v & \left(v_{\Delta \delta} - v^*\right)\big/\Delta \delta & \left(v_{\Delta \alpha} - v^*\right)\big/\Delta \alpha & \left(v_{\Delta \dot{\alpha}} - v^*\right)\big/\Delta \dot{\alpha} \\
\left(\delta_{\Delta v} - \delta^*\right)\big/\Delta v & \left(\delta_{\Delta \delta} - \delta^*\right)\big/\Delta \delta & \left(\delta_{\Delta \alpha} - \delta^*\right)\big/\Delta \alpha & \left(\delta_{\Delta \dot{\alpha}} - \delta^*\right)\big/\Delta \dot{\alpha} \\
\left(\alpha_{\Delta v} - \alpha^*\right)\big/\Delta v & \left(\alpha_{\Delta \delta} - \alpha^*\right)\big/\Delta \delta & \left(\alpha_{\Delta \alpha} - \alpha^*\right)\big/\Delta \alpha & \left(\alpha_{\Delta \dot{\alpha}} - \alpha^*\right)\big/\Delta \dot{\alpha} \\
\left(\dot{\alpha}_{\Delta v} - \dot{\alpha}^*\right)\big/\Delta v & \left(\dot{\alpha}_{\Delta \delta} - \dot{\alpha}^*\right)\big/\Delta \delta & \left(\dot{\alpha}_{\Delta \alpha} - \dot{\alpha}^*\right)\big/\Delta \alpha & \left(\dot{\alpha}_{\Delta \dot{\alpha}} - \dot{\alpha}^*\right)\big/\Delta \dot{\alpha}
\end{bmatrix}
\tag{3.17}
$$

The four eigenvalues of this matrix represent the error that remains after one stride and can be used to quantify the stability of the fixed point. If all the eigenvalues are less than one then we can say the system converges back the fixed point and it is stable. We use the maximum eigenvalue as an indicator for stability of the fixed point.

We can use the maximum eigenvalue to find the stable range of parameters of the system. We take a known fixed point and vary one parameter while keeping all the other parameters constant and find corresponding new fixed points. The stability of these new fixed points is indicated by the maximum eigenvalue. We can plot the maximum eigenvalue of the fixed point versus any parameter giving us a range of that parameter for the model for which the model is stable. We use these parameter sweeps to compare the stable range of parameters for cases with and without ankle torque.

4. RESULTS AND DISCUSSION

4.1 How Hip and Ankle Moments Affect COM and Pitching Dynamics

For the basic template of legged locmotion (point mass on a springy leg), ankle and hip actuation would affect the COM dynamics in exactly the same way, i.e. through a force tangential to the leg. As the models grow in complexity, so does the effect of moments on the dynamics. In our model we have a rigid trunk joined to a springy leg at the hip. Here ankle moments affect COM and pitching dynamics in a different way from hip moments.
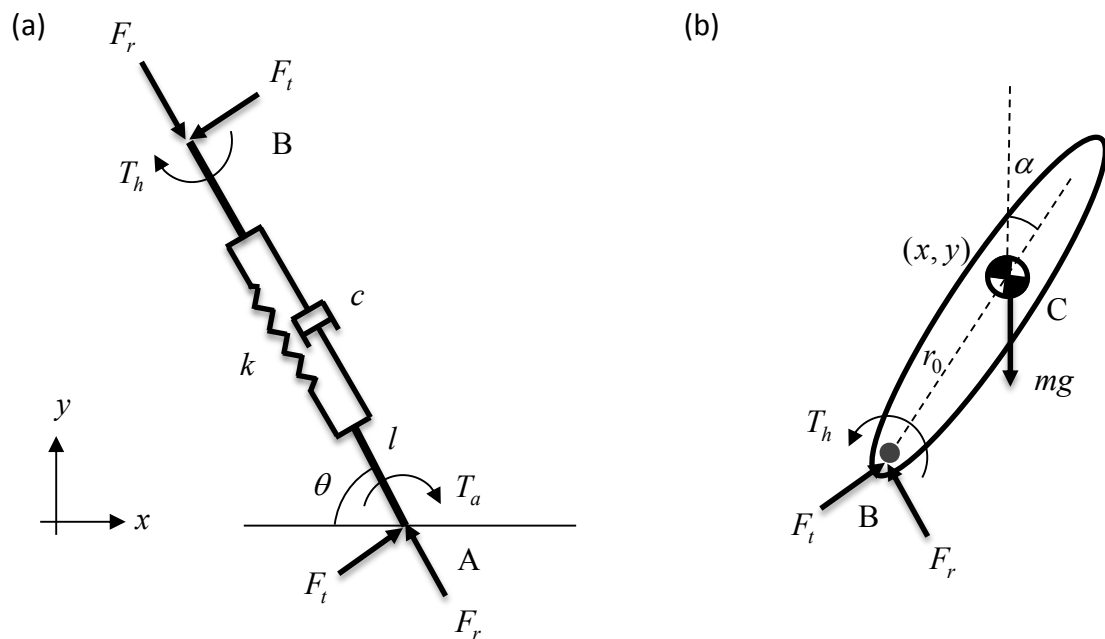

Figure 4.1. (a) Free body diagram of the massless leg. (b) Free body diagram of the trunk.

If we look at the free body diagrams again in Figure 4.1., for force balance in the leg we see that hip and ankle moments together contribute to a force tangential to the leg. An equal and opposite tangential force acts on the trunk at the hip. This tangential force has components in x and y. For force and moment balance in the trunk, the x and y forces contribute to both the translational and angular acceleration. Hence, both the hip and ankle moments contribute to COM and pitching dynamics through a force tangential to the leg. However, the equal and opposite hip moment on the trunk also contributes directly to the angular acceleration. This is also visible in the equations of motion, if we present them in terms of hip and ankle moments.

$$m\ddot{x} = \frac{(T_h + T_a)}{l}\sin\theta - F_r\cos\theta \tag{4.1}$$

$$m\ddot{y} = \frac{(T_h + T_a)}{l}\cos\theta + F_r\sin\theta - mg \tag{4.2}$$

$$I\ddot{\alpha} = \frac{(T_h + T_a)}{l}r_0\sin(\alpha - \theta) - F_r r_0\cos(\alpha + \theta) - T_h \tag{4.3}$$

To summarize, hip and ankle moments contribute to COM and pitching dynamics in different ways. While hip and ankle moments together contribute to both COM and pitching dynamics through force components, hip moments also contribute to pitching dynamics directly. Hip and ankle moments contributing in different ways could also be interpret as hip and ankle moments serving different roles in running. In humans, we would expect the hip and ankle moments to serve different roles in running. In previous modeling and robotics we have seen that hip moments are sufficient to stabilize both COM and pitching dynamics. While in theory it is also possible to stabilize both COM

and pitching dynamics with just ankle moments, we can see from the equations that hip moments can contribute more directly to pitching stabilization, making it easier to control pitching stability through simple feedback. Controlling upped body pitching with the ankle would require 8 times the ankle moments as hip moments [3]. We can hypothesize that the role of hip moments is to directly stabilize COM and pitching dynamics, and the role of ankle moments is to improve the quality of stability.

It is worth mentioning that, while this simplified model is still far away from human running, the major points discussed in this section would still apply to an anatomically accurate model. Firstly, the hip moments will still have a direct contribution to the pitching stability. Secondly, an anatomically accurate model with all the added joints and inertias would only make the effect of hip and ankle moments on COM and pitching stability more different. Just like going from a point mass to a rigid trunk did for this model.

4.2   Stable Periodic Solutions

In this section we show a stable periodic solution for the model at a running speed of 4m/s with human-like parameters for zero ankle torque. Then, keeping all other parameters same we add an ankle torque while also increasing the leg damping to compensate for the increased energy input and find a corresponding stable periodic solution. We compare those fixed points on qualitative stability, stable parameter range and step perturbations.

We use human-like values for the parameters that are used in previously conducted analysis on trunk pitching SLIP models [24,25] and are based on experimental studies. The parameters are shown in Table 4.1.

Table 4.1. Model Parameters for zero ankle torque.

Parameter	Symbol	Value
Mass	m	75 kg
Moment of inertia	I	5 kgm^2
Initial leg length	l_0	0.9 m
Leg stiffness	k	20 kN/m
Distance hip-COM	r_0	0.1 m
Reference pitching angle	α_r	2°
Proportional gain	K_p	220 Nm/rad
Derivative gain	K_d	2.5 Nms/rad
Landing angle	β	68.8°
Gravity	g	9.81 m/s^2
Leg Damping	c	25.6 Ns/m

Experimental tests on subjects running at 4m/s showed peak ankle moment between 175 to 250 Nm [6]. Keeping all the other parameters same we add a constant ankle torque (T_a) of 200 Nm which gives us a stable solution at a leg damping (c) value of 948.3 Nm/s. We have an increased leg damping value to compensate for the additional energy input. The corresponding fixed points are shown in Table 4.2.

Table 4.2. Model fixed points.

State variables	Without ankle torque	With ankle torque
v^*	4 m/s	4 m/s
δ^*	8.18°	10.2°
α^*	4.19°	4.74°
$\dot{\alpha}^*$	-6.47°/sec	5.56°/sec

We see a huge increase in leg damping value to compensate for the increased energy input. It would be interesting to see how this affects the energetic cost of the model in comparison to the human energetic cost. We discuss this in the next section.

4.3 Energetic Cost

The mechanical energy per stride, mass and distance travelled has been experimentally observed for human subjects walking at 1.4 m/s to be 1.09 J/m.kg per stride [26]. We can find a the mechanical energy per stride mass and distance travelled for our model by using the relation -

$$E.C. = \frac{T_a \Delta\theta + T_h \Delta\alpha}{m\Delta x} \qquad (4.4)$$

The energetic cost without ankle torque is 0.002 J/m.kg per stride and with ankle torque is 1.77 J/m.kg per stride for a running speed of 4m/s. Interestingly, the energetic cost with ankle moments is much closer to the human energetic cost. A larger energy input with a larger leg damping value better portrays human locomotion.

4.4   Qualitative Stability Benefits of Basic Ankle Actuation

We plot the basin of attractions for the two cases to compare their qualitative stabilities. Since there are four state variables $(v, \delta, \alpha, \dot{\alpha})$, we plot two sections of the basin corressponding to the translational and rotational variables. Figure 4.2. shows the plots of the (v, δ) basin of attraction
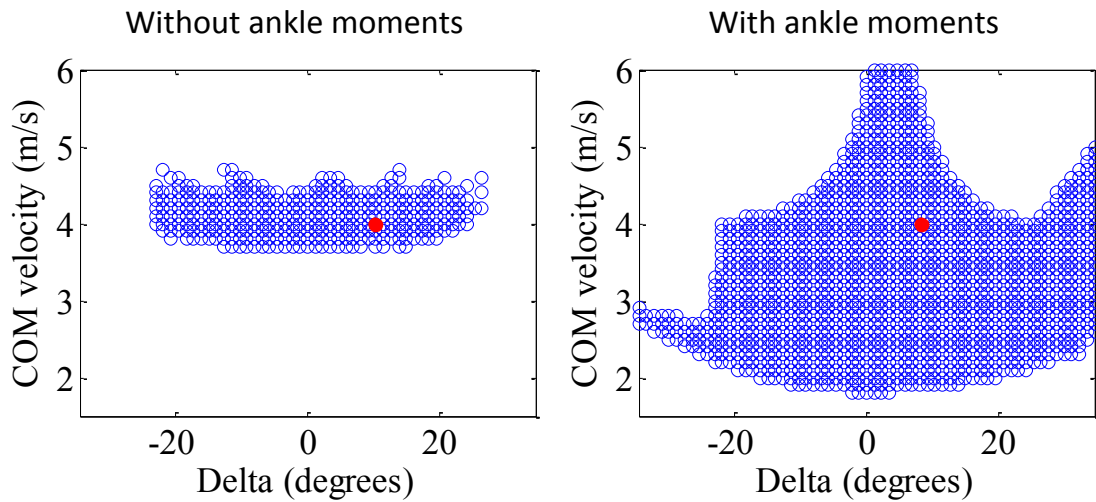
Figure 4.2. (v, δ) basin of attraction of the model without ankle torque (left), and with ankle torque (right).

The model with ankle torque shows a significantly larger basin of attraction, especially for velocity magnitude perturbations. The $(\alpha, \dot{\alpha})$ basin of attraction is plotted in Figure 4.3. Surprisingly, we see a similar increase in size of the $(\alpha, \dot{\alpha})$ basin of attraction which we associate with pitching stability. Adding ankle torque with an accompanied increase in the leg damping has a significant impact even on the pitching dynamics even though the hip torque is still roughly the same, along with all other parameters. This shows the coupled nature of the dynamics of this model
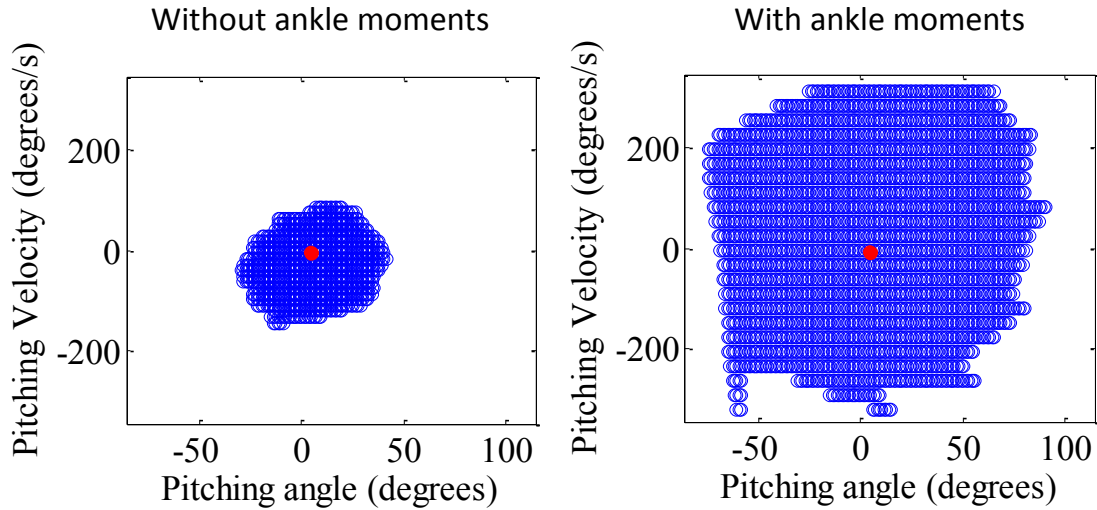
Figure 4.3. $(\alpha, \dot{\alpha})$ basin of attraction of the model without ankle torque (left), and with ankle torque (right).

4.5 Sensitivity of Stability to Control Parameters

In this section we compare the range of control parameters K_p, α_r, K_d, and T_a for which these models have stable solutions. Starting from the stable fixed point shown earlier, we vary the chosen parameter while keeping all other parameters constant and find the corresponding new fixed points. Using the maximum eigenvalue as an indicator for the new fixed point we can plot the stability of the fixed points versus the parameter being varied. This gives us the range of parameters for which the model is stable and is an indicator of the robustness of the model to parameter variation.

We see in Figure 4.4 (a) that addition of ankle moments increases the range proportional gain K_p for stable solution by nearly 20 times. We see a similar increase in parameter range for reference pitching angle α_r and derivative gain K_d.
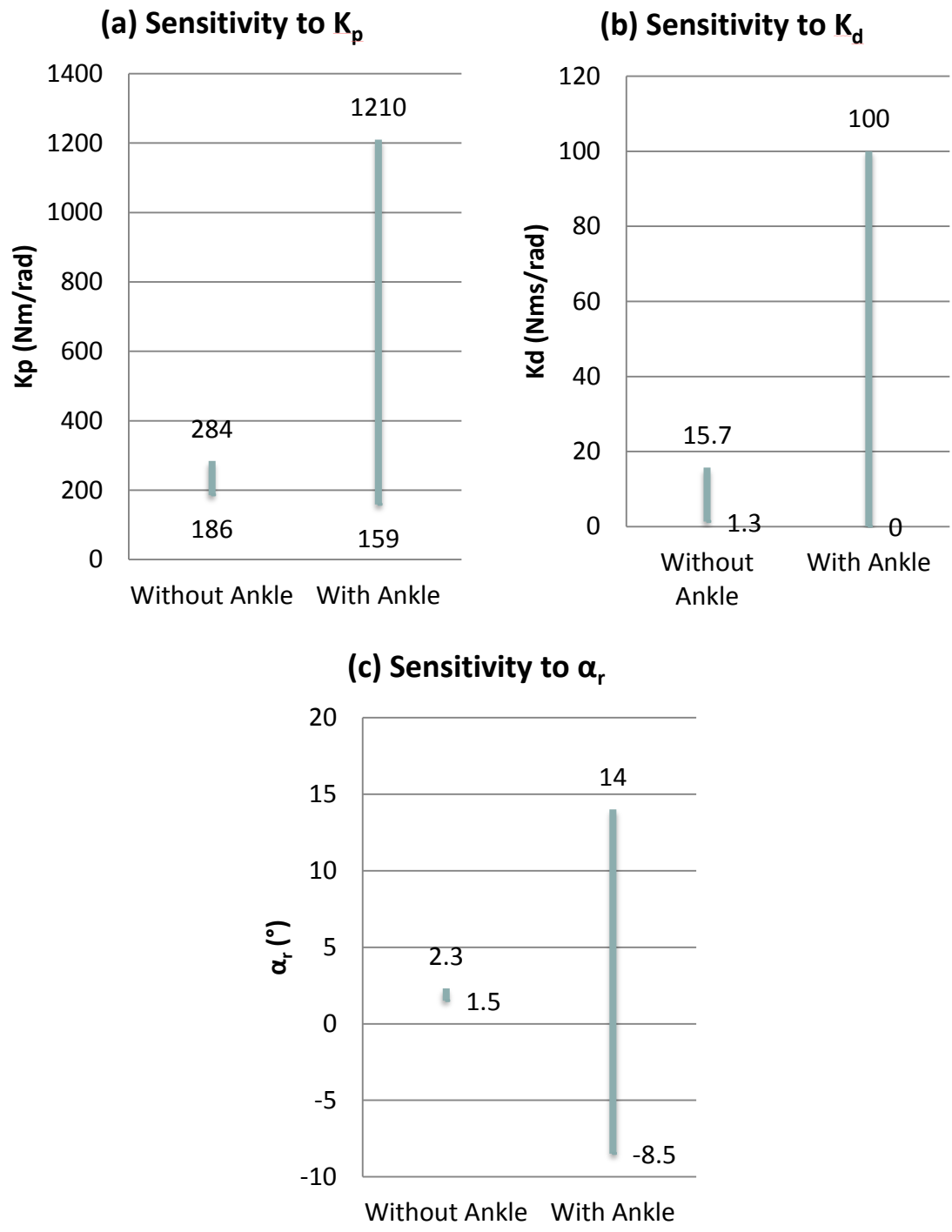
Figure 4.4. Comparison of range of stable parameters based on the maximum eigenvalue. (a) Compares the range of K_p, (b) compare the range of K_d, (c) compares the range of α_r

Surprisingly, we see that adding ankle moments widens the range of hip control parameters. This could be because without ankle moments, the hip moments had to stabilize COM and pitching dynamics alone, boxing the control parameters into a narrow range around the current fixed point. The addition of ankle moments can free us to choose from a much wider range of hip control parameters. This could be beneficial for designing the hip moments in robots.

4.6   Sensitivity of Stability to Leg Parameters

Similar to the earlier section, here we compare the range of stable parameters like k, β, and c for which the model has stable solutions. Stable range of leg stiffness is compared in Figure 4.5 (a). We see that both cases present stable solutions for a similar range of leg stiffness which falls in the human-like range of leg stiffness [15]. Both cases are relatively sensitive to variation in landing angle, but the case with ankle torque appears to be more sensitive as shown in Figure 4.5 (c). This could be because leg landing angle directly influences the energy input for constant ankle moments. Leg landing angle is a parameter that is easily controlled in flight and should not pose a design problem. Without ankle actuation the model is stable for a very small range of leg damping and with ankle actuation it is stable for a very wide range of leg damping values as shown in Figure 4.5 (b). Varying the leg damping value primarily changes the velocity in the new stable solution. This property could have an interesting application in robotics where a variable damper can be used at the leg to allow changing velocities. Increasing damping can also be used to improve the time response to perturbations

(a) Sensitivity to k

(b) Sensitivity to c
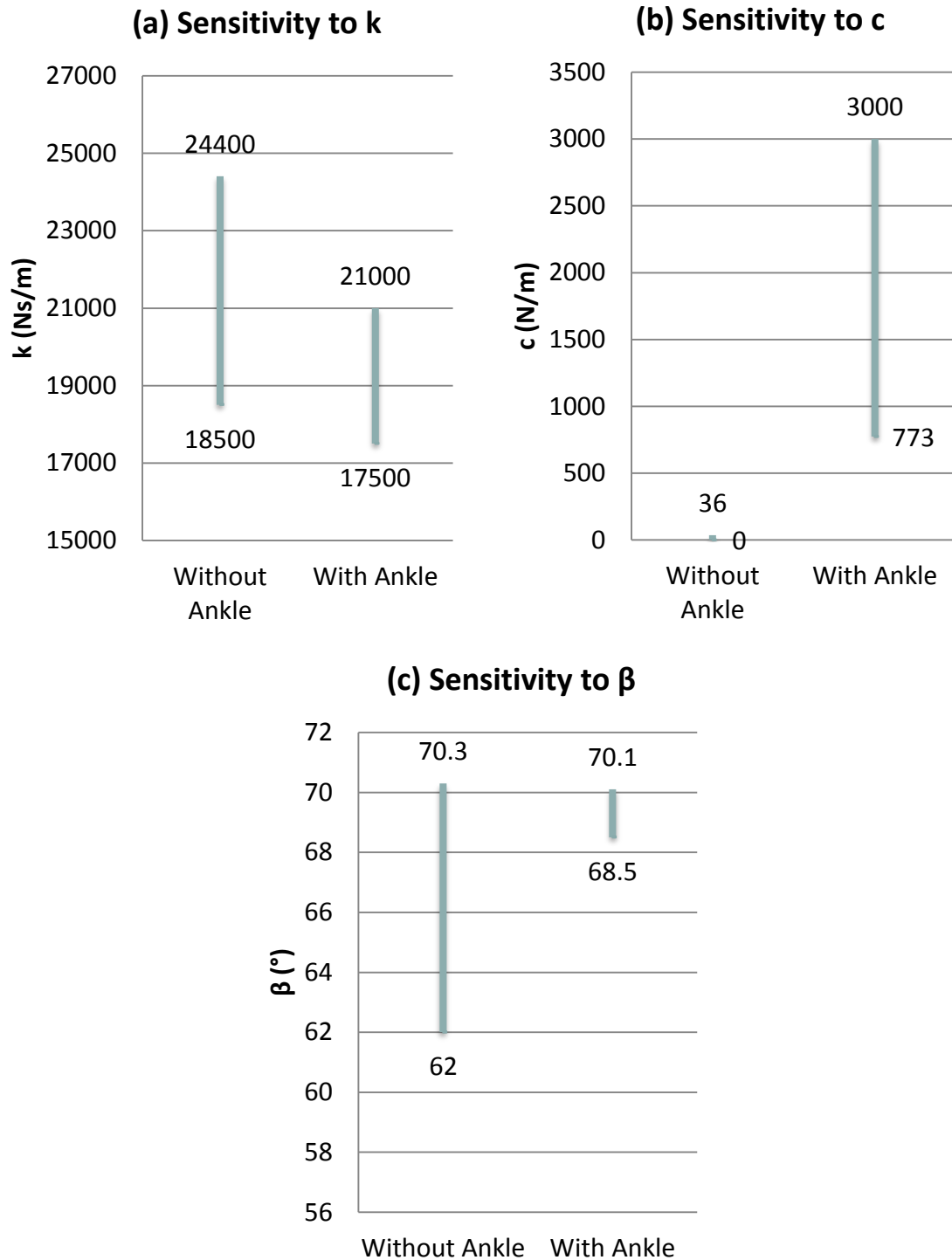

(c) Sensitivity to β

Figure 4.5. Comparison of range of stable parameters based on the maximum eigenvalue. (a) Compares the range of k , (b) compare the range of c , (c) compares the range of β

4.7   Sensitivity of Stability to Mass and Moment of Inertia

Similar to the earlier section, here we compare the range of mass m and moment of inertia I for which the model has stable solutions while keeping all other parameters constant. Although in humans, mass and moment of inertia are parameters that are related to each other in some way, an experimental study showed that their relation is complicated and involves other parameters too like trunk dimensions [27]. We perform this sensitivity analysis, purely to see the effect of ankle moments on regions of stability in line with our earlier analysis. Stable range of body mass is shown in Figure 4.6.(b). The model without ankle torque has stable solutions for a mass range of around 51 to 85 kg whereas the model with ankle torque has a range of around 1 to 86 kg. We see the model with ankle moments is stable for much lower masses. The comparison of moment of inertia is an interesting one, because in the case on the model with ankle moments, as the moment of inertia becomes infinite, the model exactly resembles a hip-actuated SLIP model. This is because in the hip-actuated SLIP model considers a point mass and ankle moments affect the COM dynamics in exactly the same way as hip moments. So we theoretically expect the model with ankle moments to have no upper cap on the range of moment of inertia for stable solutions. We see exactly that, however, the plot of the stable range of moment of inertia for the case with ankle moments is cut off at 20 kgm^2 so that we can focus on the lower cap of moment of inertia. Figure 4.6.(a) show the range of stable moment of inertia without and with ankle moments respectively. We see that the model without ankle moments is stable between 1.6 and 10.5 kgm^2 and the mode with ankle moments is stable from 0.6 kgm^2 onwards. An experimental study on 26 male subjects [27] showed a variation in trunk moment of inertia of 1 to 3.6 kgm^2. Note that

this is only the 'trunk' moment of inertia and it does not include the hands, neck and head. With that in mind, we can say that the model without ankle torque is stable for the entire human range plus a bit more. The model with ankle moments is stable for a much wider range of moment of inertias.
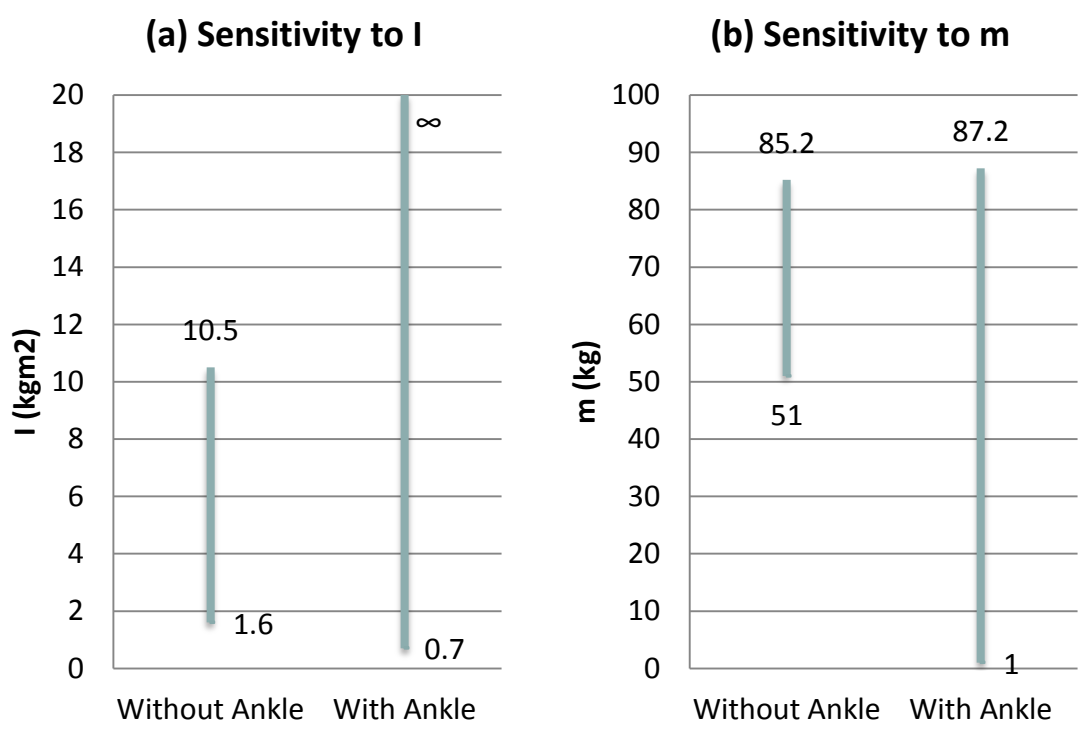
Figure 4.6. Comparison of range of stable parameters based on the maximum eigenvalue. (a) Compares the range of m, (b) compare the range of I.

4.8   Sensitivity to Velocity and Stability of Fixed Points at Other Velocities

Similar to earlier parameter sensitivity analysis, this time we vary velocity while keeping all the other parameters same and find new stable solutions. However, earlier when we varied a parameter we would find new initial state variables as the corresponding stable solution. Here, as the parameter we are varying is itself a state

variable, we find new values of the other three state variables with damping for the new stable solution.
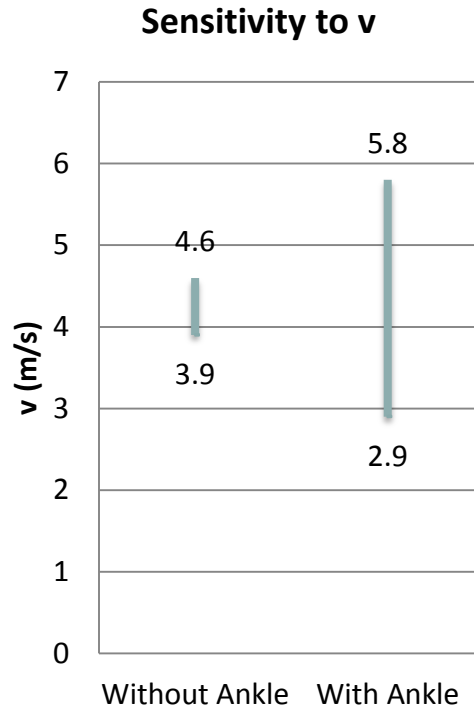
Sensitivity to v

Figure 4.7. Plot showing maximum eigenvalue versus variation in velocity for the model (a) without ankle torque and (b) with ankle torque.

We find there is a wider range of velocities with stable solutions with ankle torque than without, as shown in Figure 4.7. We were unable to find stable solutions for lower running velocities without ankle moments for human-like parameters. With ankle moments the model is closer to the lower extreme velocity for a running gait.

Even at lower velocities, we see that the model with ankle moments displays large perturbation stability, as shown by the basin of attraction in Figure 4.8. The parameters for this stable solution are, $k = 20000$ N/m, $m = 75$ kg, $K_p = 350$ Nm/rad, $g = 9.8 \ m/s^2$,

$K_d = 20$ Nms/rad , $l_0 = 0.9$ m , $r_0 = 0.1$ m , $c = 1878.9$ Ns/m , $I = 5$ kgm^2 , $\alpha_r = 3°$,

$\beta = 72°$, $T_a = 160$ Nm . The fixed point values of the state variables (v, δ, α, $\dot{\alpha}$) are 3
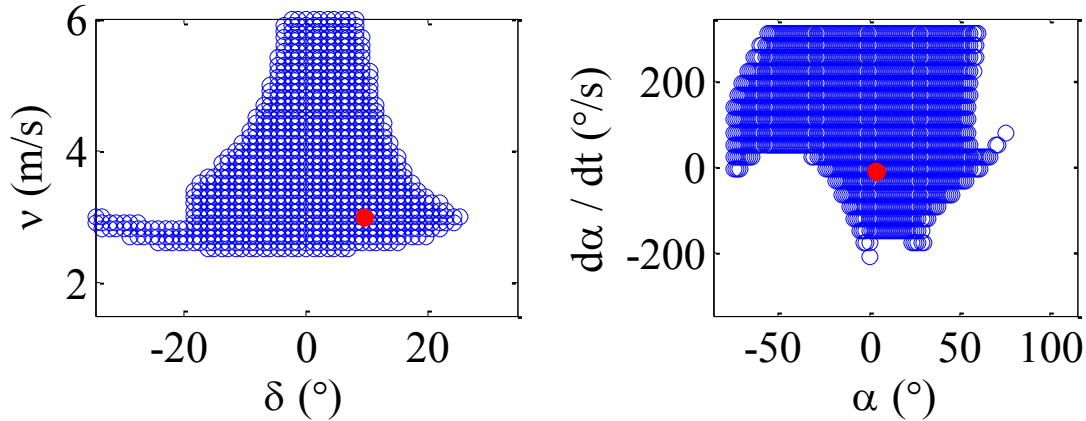
m/s, 9.37°, 3.6°, and 8.7°/s

Figure 4.8. Basins of attraction of the model with ankle torque for a velocity of 3 m/s, (v, δ) (left) and (α, $\dot{\alpha}$) (right).

4.9   Stability of Other Solutions and Sensitivity to Ankle Moments

In this section we check the stability of some other fixed points for the model with ankle moments. The sensitivity comparisons showed an overall increase in the range of stable parameters and it would be interesting to check the quality of stability of some other fixed points and see if the pattern repeats itself.

4.9.1   Stability of Locomotion at the Mid-point of the Stable Parameter Range

The earlier fixed point we analyzed had human-like parameters for those parameters which are directly relatable to humans and other parameters like hip control parameters, leg stiffness, damping and landing angle were based on a stable solution of a previously studied model with only hip moments. It would be interesting to see the stability of a

fixed point where those other parameters are chosen for the case with both hip and ankle

moments. We are not equipped to choose the optimum set of parameters for any case as

there are too many parameters and their effect is through a set of coupled second order

nonlinear differential equations. However, we know that the fixed points for parameters

that are at the edge of the stable range, in general have smaller basins of attraction.

Table 4.3. Model parameters for the model with ankle moments, where
$K_p, K_d,\ \alpha_r,\ k,\ c,$ and β are chosen by locating the middle of the earlier analyzed stable
range.

Parameter	Symbol	Value
Mass	m	75 kg
Moment of inertia	I	5 kgm^2
Initial leg length	l_0	0.9 m
Leg stiffness	k	19250 N/m
Distance hip-COM	r_0	0.1 m
Reference pitching angle	α_r	2.75°
Proportional gain	K_p	684.5 Nm/rad
Derivative gain	K_d	50 Nms/rad
Landing angle	β	69.3°
Gravity	g	9.81 m/s^2
Leg Damping	c	1047.5 Ns/m

Hence, we choose those other parameters by locating the middle of the stable range

we analyzed earlier. We do not claim this to be an 'optimized' parameter set, but this

parameter set is more likely to have a stable fixed point. For the parameters displayed in Table 4.3., the fixed point values of the state variables $(v, \delta, \alpha, \dot{\alpha})$ are 4 m/s, 7.47°, 2.69°, and $-6.04°/s$. We plot the basin of attraction for this fixed point in Figure 4.9. We see that the (v, δ) is similar to the earlier fixed point with ankle moments, however the $(\alpha, \dot{\alpha})$ basin of attraction is much larger.
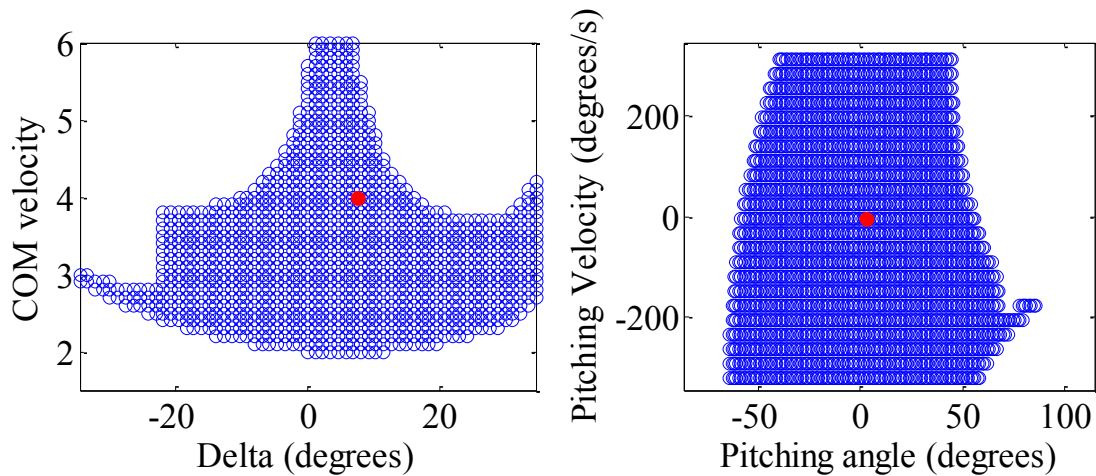
Figure 4.9. (v, δ) Basin of attraction (left) and $(\alpha, \dot{\alpha})$ basin of attraction (right) for parameters chosen based on the sensitivity study.

4.9.2 Effect of Varying Ankle Moments

It would be interesting to see the effect varying ankle moments has on the basins of attraction. Keeping all the other parameters same as the previous study, we vary ankle moments and damping and find the corresponding fixed points. The basins of attraction for ankle moments varying from 100 Nm to 300 Nm are plotted in Figure 4.10.
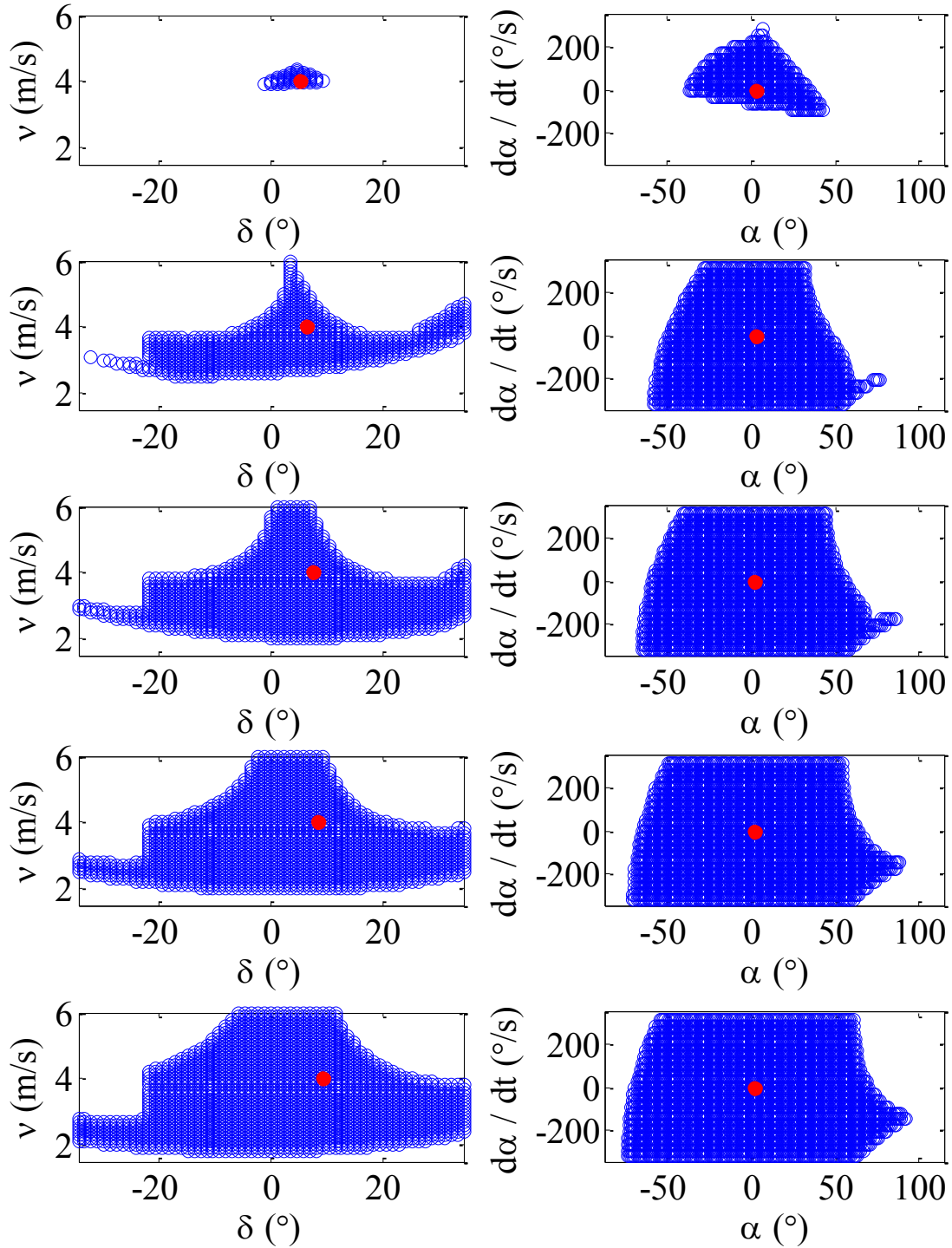
Figure 4.10. $(v,\ \delta)$ Basin of attraction (left) and $(\alpha,\ \dot{\alpha})$ basin of attraction (right) as we vary the value of ankle moments from 100 Nm (above) to 300Nm (below) in increments of 50 Nm.

We see that the area of the basin of attraction increases as we increase ankle moments. The rate of increase is faster near 100 Nm and it slows down as we increase ankle moments. If we keep varying the leg damping value to compensate for the ankle moments, for a COM velocity of 4m/s we were able to find stable solutions for ankle moments from 98 Nm to 1888 Nm as shown in Figure 4.11. The experimentally determined peak ankle moments in humans ranged from 175-340 Nm for running to sprinting speeds [6]. This goes much beyond that human range and large ankle moments can be used in robotics to improve the response to perturbations.
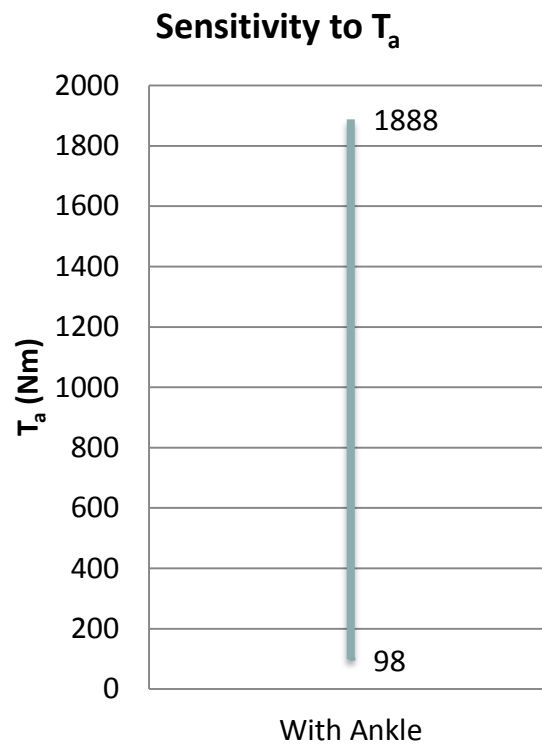

Figure 4.11. Stable range of ankle moments.

4.9.3   Stability Comparisons at Different Velocities

We have analyzed a couple of fixed points at 4 m/s, now we will compare the qualitative stability of fixed points at 5, and 6 m/s to see if we observe a similar increase in basins of attraction. As we saw earlier that we could not find any stable solutions without ankle moments for a velocity of 3 m/s for human-like parameters, hence we are comparing fixed point at higher velocities.

For a running velocity of 5 m/s, for the case without ankle moments, we find a stable solution for the parameters, $k = 20000$ N/m, $m = 75$ kg, $K_p = 200$ Nm/rad, $g = 9.8 \, m/s^2$, $K_d = 10$ Nms/rad, $l_0 = 0.9$ m, $r_0 = 0.1$ m, $c = 23.79$ Ns/m, $I = 5$ kgm^2, $\alpha_r = 2°$, $\beta = 67.5°$. The fixed point values of the state variables (v, δ, α, $\dot{\alpha}$) are 5 m/s, 5.07°, 4.42°, and -4.87°/s. For the case with ankle moments, we add ankle moments of $T_a = 200$ Nm and increase the damping value to $c = 703.76$ Ns/m, to compensate for the increased energy input. The new fixed point values of the state variables (v, δ, α, $\dot{\alpha}$) for the case with ankle moments are 5 m/s, 6.45°, 5.33°, and -5.61°/s. Notice that we have changed some of the parameters from the previous parameters to increase the sampling space. The basins of attraction for these points are compared in Figure 4.12. We see a similar increase in both the translational and rotational basins of attraction.
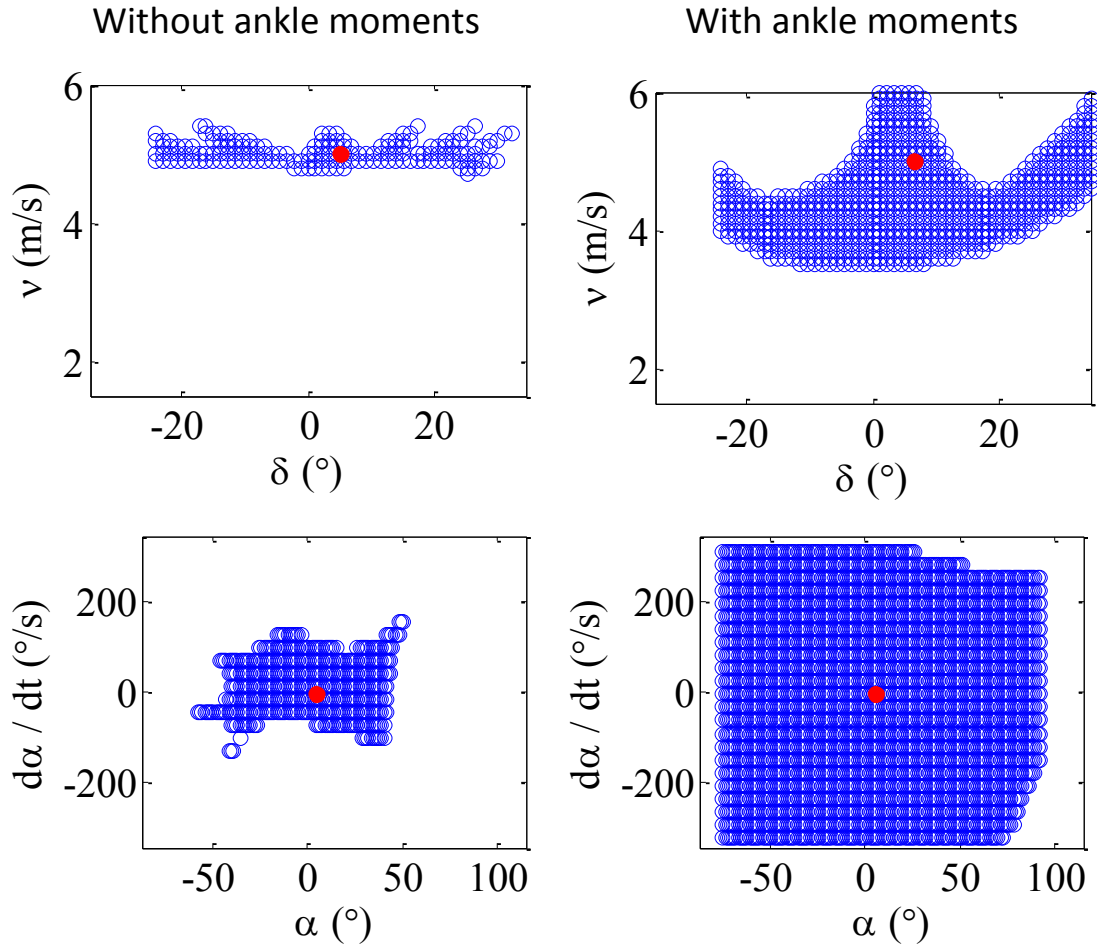
Figure 4.12. Comparison of basins of attraction for a running velocity of 5 m/s.

For a running velocity of 6 m/s, for the case without ankle moments, we find a stable solution for the parameters, $k = 20000$ N/m , $m = 75$ kg , $K_p = 200$ Nm/rad , $g = 9.8\ m/s^2$, $K_d = 10$ Nms/rad , $l_0 = 0.9$ m , $r_0 = 0.1$ m , $c = 53.94$ Ns/m , $I = 5$ kgm^2 , $\alpha_r = 2°$, $\beta = 63.5°$. The fixed point values of the state variables ($v,\ \delta,\ \alpha,\ \dot{\alpha}$) are 6 m/s, 9.24°, 13.37°, and -5.86°/s. The case with ankle moments was found to be unstable for that landing angle and we change it to $\beta = 67.5°$. We will discuss this in more detail in the next sub-section. With the new landing angle, we add ankle moments of

$T_a = 250$ Nm and increase the damping value to $c = 823.02$ Ns/m, to compensate for the increased energy input. The new fixed point values of the state variables (v, δ, α, $\dot{\alpha}$) for the case with ankle moments are 6 m/s, 5.19°, 7.51°, and -4.98°/s. The basins of attraction for these points are compared in Figure 4.13. Again we see a similar increase in the basins of attractions. The translational basin of attraction is particularly larger.
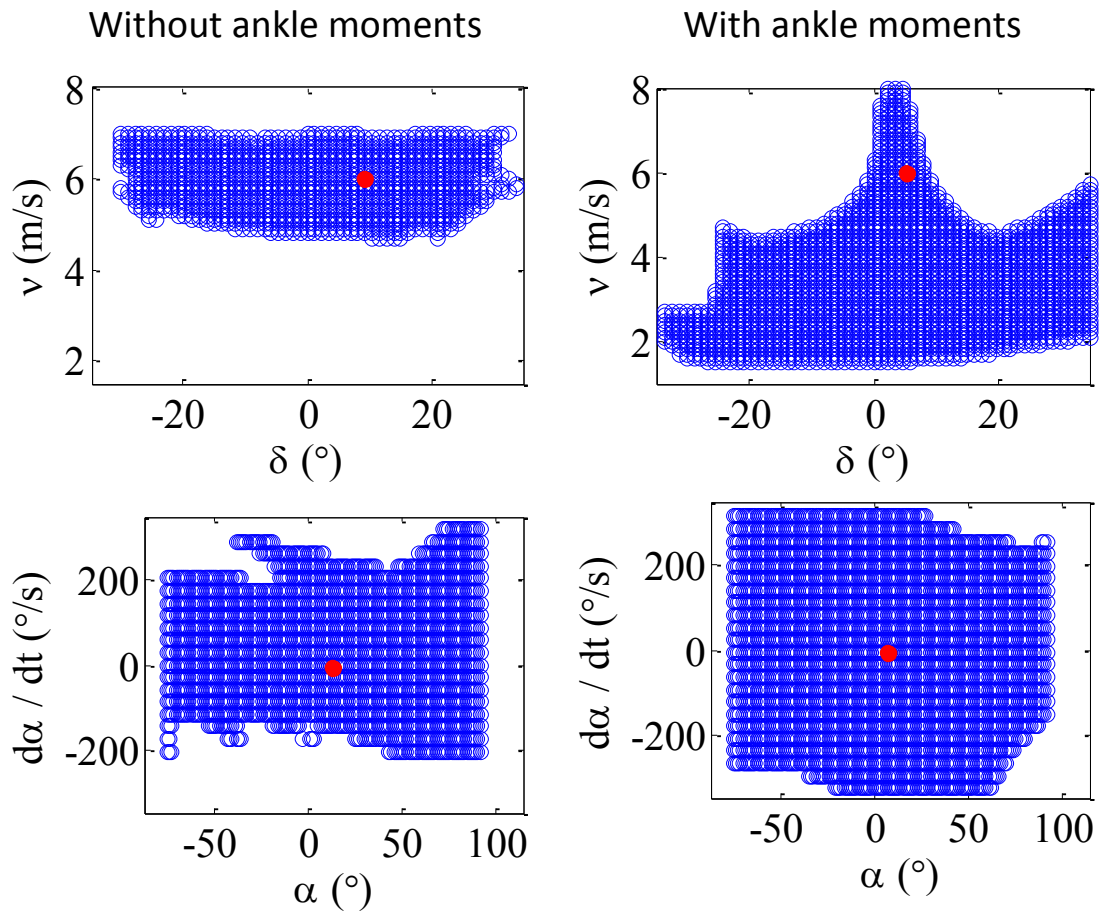

Figure 4.13. Comparison of basins of attraction for a running velocity of 6 m/s.

4.9.4 Stability and Landing Angles

We saw in the previous sections that the case with constant ankle moments is more sensitive to landing angle selection than without ankle moments. Then in the previous

sub-section we saw that as we increase the velocity the overlap of stable range of landing angles reduces. For a running velocity of 6 m/s we saw that the case without ankle moments was stable at lower landing angles than with ankle moments. For those parameters, we see that just adding ankle moments and damping does not improve stability but rather leads to instability. The cases with and without ankle moments are two different systems and have different range of stable solutions, which sometimes do not overlap. Here we explore that parameter space for a running speed of 6 m/s a bit further. We find that for those parameters both cases have a fixed point at a landing angle of 64°. It would be interesting to compare the basins for these parameters as this would be on the edge of the stable range of landing angles for the case with ankle moments. Consider the parameters , $k = 20000$ N/m , $m = 75$ kg , $K_p = 200$ Nm/rad , $g = 9.8 \ m/s^2$, $K_d = 10$ Nms/rad , $l_0 = 0.9$ m , $r_0 = 0.1$ m , $c = 40.19$ Ns/m , $I = 5$ kgm^2 , $\alpha_r = 2°$, $\beta = 64°$. The fixed point values of the state variables (v, δ, α, $\dot{\alpha}$) are 6 m/s, 8.15°, 9.6°, and -5.56°/s. For the case with ankle moments, we add ankle moments of $T_a = 250$ Nm and increase the damping value to $c = 561.04$ Ns/m, to compensate for the increased energy input. The new fixed point values of the state variables (v, δ, α, $\dot{\alpha}$) for the case with ankle moments are 6 m/s, 7.67°, 12.47°, and -6.76°/s. The basins of attraction are compared in Figure 4.14. We find that in this case adding ankle moments decreases the stability of the solution. We expect this because the solutions tend to become less stable as we move towards the edge of the stable parameter region. This goes to show that both systems have their own stable parameter space and when they do not overlap or overlap thinly adding ankle moments will reduce stability or lead to instability. This is

particularly visible in the case of landing angle and leg damping. The other parameters have a sizeable overlap in parameter space. In moving from just hip moments to hip and ankle moments, we have to be careful in choosing the leg damping and leg landing angle values such that they are suited to the case with ankle moments. Leg landing angle is easily controlled in flight so this should not be a design problem.
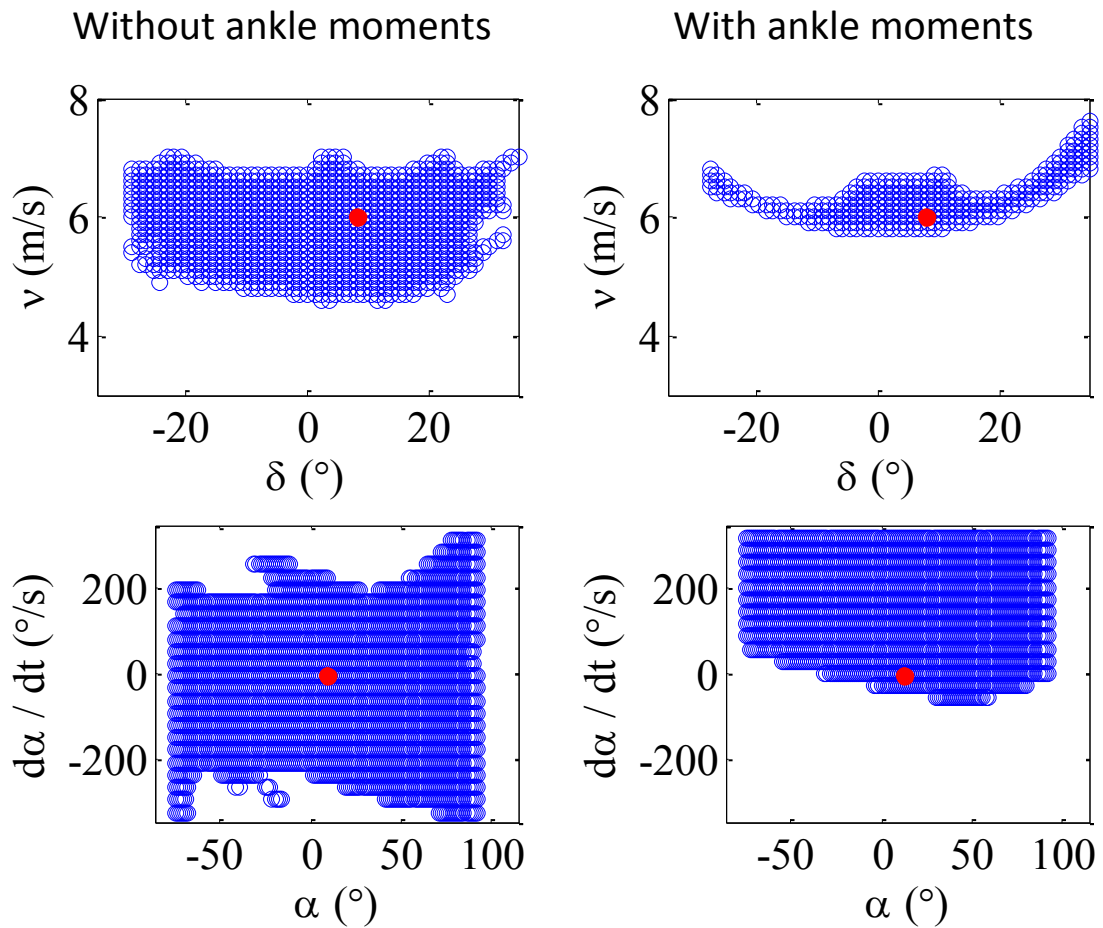

Figure 4.14. Comparison of basins of attraction for a running velocity of 6 m/s and the same leg landing angle of 64°.

5. SUMMARY

The theoretical modeling and simulation analysis presented here helped us determine more about the differentiated roles that ankle and hip moments play to affect the COM and pitching dynamics of locomotion. The governing equations of our model demonstrated explicitly that hip moments are better suited for controlling upper body balance and that ankle moments can only affect COM and pitching dynamics indirectly.

This theoretical locomotion model and its governing equations were studied further using numerical simulation. Two cases were compared, one with ankle moments and one without which represented the previous state of art of hip based models and dynamics robots. Although, the model with ankle moments required a significantly larger leg damping value to maintain the same speed as the model without ankle moments, its energetic cost was much closer to the energetic cost in humans than without ankle moments. It was also found that the model with ankle moments had significantly larger basins of attraction. In addition, the model with ankle moments had stable solutions for a wider range of parameters with possible applications extending well beyond the human range of parameters. The leg landing angle was an exception as it was shown to be a sensitive parameter for the model with ankle moments. The model with ankle moments also had stable solutions for a wider range of COM velocities, with the lower end of the range getting closer to the minimum threshold velocity of humans in running gait, which

implies that a robot with an ankle moment could run over a wider range than one that is based purely on a hip-based actuation method.

When studying the effect of varying the magnitude of ankle moment, we found that the basins of attraction enlarged in a roughly proportionate manner with increasing ankle moments so long as the leg damping was also increased to compensate the increased energy input and maintain a steady speed. A similar stability comparison was carried out with different parameters at different running velocities to see if the improvements in basins of attraction repeated. It was found that for some cases the stable range of leg landing angle values did not overlap for the cases with and without ankle moments. Simply adding ankle moments and leg damping to these cases had the opposite effect and made the model unstable. However, leg landing angle is a parameter that is easily controlled in flight and if it is adjusted for, then the model with ankle moments generally showed an improvement in the basin of attraction, an important measure of stability.

Overall, the results of this study showed that for the locomotion model we studied, ankle moments play a role in improving the response to perturbations and enlarging the stable regions. While this model is still far from accurately representing human running, the results of this study can provide some insights about human running which could form the basis of more focused and detailed studies in the future. The main current benefit of this model is to help extend the existing theoretical knowledge of hip-based springy-leg models and dynamic robots towards models and robots that include an ankle, with the expected benefits of increased stability.

The model analyzed here approximates a robot with a rigid trunk, a telescoping leg with a spring and damper inside and a small foot as shown in Figure 5.1. The trunk would

contain motors to actuate the leg at the hip joint with PD controlled moments. The lower half of the telescoping leg would contain the actuators to generate a constant 'ankle' moment. The results of this thesis can be used towards the design of such a robot. From the results, we know the stable range of parameters to design the robot and the kind of response to perturbations to expect from it.
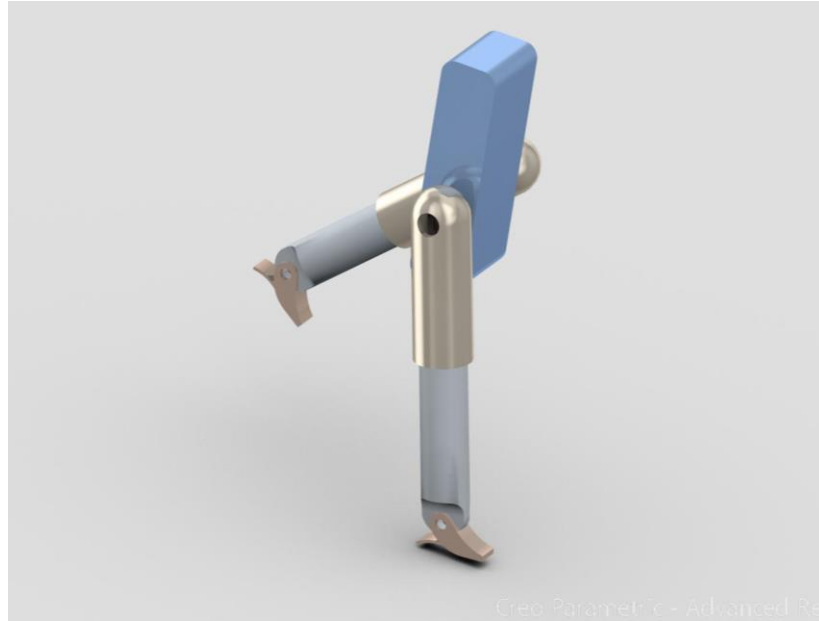

Figure 5.1. An artistic representation of a robot that represents our model.

The proposed robot could also be used to experimentally verify the predictions of the model. For example, we could include a damper with variable damping coefficient and a variable ankle moment, and measure the systems response to perturbations to see when the robot can sustain the largest perturbations.

6. FUTURE WORK

This study presented a simple step forward towards understanding bipedal locomotion. As with all simplified models, there are certain limitations, and in this section we list out next possible steps forward.

6.1   Ankle Moment Patterns or Control Strategies

This study focused on analyzing the effect of adding the simplest ankle moment pattern. It could be interesting to see how using the human ankle moment pattern might affect the stability of human running in direct comparison with this study. It could also be interesting to explore specific control strategies which relate to the role of the human ankle.

6.2   Ankle Joint

In this study we used a simplified model that did not consider a separate ankle segment that is free to lift off the ground, and the different phase transitions that come along with it (CP, CD, and PP). Adding an ankle joint while keeping the rest of the leg as a spring might be the next modeling step. The conclusions from such a study may directly show the effect of these foot contact phases when compared to this study.

6.3   Applying Ankle Moments to Segmented Leg Models

Previously studied hip-actuated segmented leg models faced a critical problem when the leg segments reached the aligned position "toggle" position [28]. This "toggle" position was shown to cause a singularity in the vertical ground reaction force causing the system to crash. This singularity occurred because the hip torque was unbalanced in the "toggle" position. Adding an ankle moment just like in our model may balance the hip torque under certain conditions. We discuss such a model in more detail in the Appendix.

6.4   Testing the hypothesis with similar robots

We have seen that there are robots that are able to stabilize COM and pitching dynamics with hip moments alone, as predicted by the hip-actuated trunk pitching models. A robot which extends upon these previous hip-driven robots, but with additional ankle moments, could be constructed to test the hypothesis presented in this study. Such a robot is discussed in more detail in the previous section.

LIST OF REFERENCES

LIST OF REFERENCES

[1]   Winter, D. A., 2009, Biomechanics and Motor Control of Human Movement, John Wiley & Sons.

[2]   Winter, D. A., and Bishop, P. J., 1992, "Lower Extremity Injury: Biomechanical factors associated with chronic injury to the lower extremity," Sport. Med., **14**(3), pp. 149–156.

[3]   Winter, D. A., Ruder, G. K., and MacKinnon, C. D., 1990, "Control of balance of upper body during gait," Multiple Muscle Systems, J.M. Winters, and S.L.-Y. Woo, eds., Springer New York, New York, NY, pp. 534–541.

[4]   Winter, D. A., 1983, "Moments of force and mechanical power in jogging," J. Biomech., **16**(1), pp. 91–97.

[5]   Palmer, M. L. 1974-, 2002, "Sagittal plane characterization of normal human ankle function across a range of walking gait speeds."

[6]   Stefanyshyn, D., and Nigg, B., 1998, "Dynamic Angular Stiffness of the Ankle Joint During Running and Sprinting," J. Appl. Biomech., pp. 292 – 299.

[7]   Novacheck, T. F., 1998, "The biomechanics of running," Gait Posture, **7**(1), pp. 77–95.

[8]   Boccardi, S., Pedotti, A., Rodano, R., and Santambrogio, G. C., 1981, "Evaluation of muscular moments at the lower limb joints by an on-line processing of kinematic data and ground reaction," J. Biomech., **14**(1), pp. 35–45.

[9]   Arampatzis, A., Brüggemann, G.-P., and Metzler, V., 1999, "The effect of speed on leg stiffness and joint kinetics in human running," J. Biomech., **32**(12), pp. 1349–1353.

[10]   Hansen, A. H., Childress, D. S., Miff, S. C., Gard, S. A., and Mesplay, K. P., 2004, "The human ankle during walking: implications for design of biomimetic ankle prostheses.," J. Biomech., **37**(10), pp. 1467–74.

[11] Neville, N., Buehler, M., and Sharf, I., 2006, "A bipedal running robot with one actuator per leg," Proceedings 2006 IEEE International Conference on Robotics and Automation, 2006. ICRA 2006., IEEE, pp. 848–853.

[12] Hyon, S., and Emura, T., 2005, "Symmetric Walking Control: Invariance and Global Stability," Proceedings of the 2005 IEEE International Conference on Robotics and Automation, IEEE, pp. 1443–1450.

[13] Au, S. K., Dilworth, P., and Herr, H., 2006, "An ankle-foot emulation system for the study of human walking biomechanics," Proceedings 2006 IEEE International Conference on Robotics and Automation, 2006. ICRA 2006., IEEE, pp. 2939–2945.

[14] Eilenberg, M. F., Geyer, H., and Herr, H., 2010, "Control of a powered ankle-foot prosthesis based on a neuromuscular model.," IEEE Trans. Neural Syst. Rehabil. Eng., **18**(2), pp. 164–73.

[15] Holmes, P., Full, R. J., Koditschek, D., and Guckenheimer, J., 2006, "The Dynamics of Legged Locomotion: Models, Analyses, and Challenges," SIAM Rev., **48**(2), pp. 207–304.

[16] Full, R., and Koditschek, D., 1999, "Templates and anchors: neuromechanical hypotheses of legged locomotion on land," J. Exp. Biol., **202**(23), pp. 3325–3332.

[17] Blickhan, R., 1989, "The spring-mass model for running and hopping," J. Biomech., **22**(11-12), pp. 1217–1227.

[18] Richard Altendorfer, Uluc Saranli, Haldun Komsuoglu, Daniel Koditschek, H. Benjamin Brown Jr., Martin Buehler, Ned Moore, Dave McMordie, R. F., 2001, "Evidence for Spring Loaded Inverted Pendulum Running In a Hexapod Robot," Proc. Int. Symp. Exp. Robot., **Volume 271**(Experimental Robotics VII), pp. 291–302.

[19] Seipel, J., and Holmes, P., 2007, "A simple model for clock-actuated legged locomotion," Regul. Chaotic Dyn., **12**(5), pp. 502–520.

[20] Saranlı, U., Arslan, Ö., Ankaralı, M. M., and Morgül, Ö., 2010, "Approximate analytic solutions to non-symmetric stance trajectories of the passive Spring-Loaded Inverted Pendulum with damping," Nonlinear Dyn., **62**(4), pp. 729–742.

[21] Shen, Z. H., and Seipel, J. E., 2012, "A fundamental mechanism of legged locomotion with hip torque and leg damping.," Bioinspir. Biomim., **7**(4), p. 046010.

[22] Maykranz, D., and Seyfarth, A., 2014, "Compliant ankle function results in landing-take off asymmetry in legged locomotion.," J. Theor. Biol., **349**, pp. 44–9.

[23] Rao, N., Shen, Z., and Seipel, J., 2013, "Comparing Legged Locomotion With a Sprung-Knee and Telescoping-Spring When Hip Torque is Applied," Volume 7A: 9th International Conference on Multibody Systems, Nonlinear Dynamics, and Control, ASME, p. V07AT10A015.

[24] Che, Y., Shen, Z., and Seipel, J., 2013, "A Simple Model for Body Pitching Stabilization," Volume 7A: 9th International Conference on Multibody Systems, Nonlinear Dynamics, and Control, ASME, p. V07AT10A014.

[25] Maus, H.-M., Rummel, J., and Seyfarth, A., 2008, "Stable Upright Walking and Running using a simple Pendulum based Control Scheme," International Conference on Climbing and Walking RobotsInternational Conference on Climbing and Walking Robots.

[26] Winter, D. A., 1979, "A new definition of mechanical work done in human movement.," J. Appl. Physiol., **46**(1), pp. 79–83.

[27] Pearsall, D. J., Reid, J. G., and Ross, R., 1994, "Inertial properties of the human trunk of males determined from magnetic resonance imaging," Ann. Biomed. Eng., **22**(6), pp. 692–706.

[28] Rao, N. V, 2013, Analysis of an actuated two segment leg model of locomotion.